INL/RPT-23-70721-Revision-0

Assessment of Acoustic Sensor Application to Structural Health Monitoring of Reactor Components

December 2022

Joshua E Daw

Changing the World's Energy Future

Idaho National Laboratory

INL is a U.S. Department of Energy National Laboratory operated by Battelle Energy Alliance, LLC

INL/RPT-23-70721-Revision-0

Assessment of Acoustic Sensor Application to Structural Health Monitoring of Reactor Components

Joshua E Daw

December 2022

Idaho National Laboratory
Idaho Falls, Idaho 83415

http://www.inl.gov

Prepared for the
U.S. Department of Energy
Under DOE Idaho Operations Office
Contract DE-AC07-05ID14517

INL/RPT-23-70721
Revision 0

Assessment of Acoustic Sensor Application to Structural Health Monitoring of Reactor Components

Dec. 2022

M3CT-22IN0702036

Joshua Daw
Idaho National Laboratory

Morris Good, Ryan Meyer
Pacific Northwest National Laboratory

Pradeep Ramuhalli
Oak Ridge National Laboratory

Luke Breon
Electric Power Research Institute

Idaho National Laboratory

INL is a U.S. Department of Energy National Laboratory operated by Battelle Energy Alliance, LLC

INL/RPT-23-70721
Revision 0

Assessment of Acoustic Sensor Application to Structural Health Monitoring of Reactor Components

M3CT-22IN0702036

Joshua Daw
Idaho National Laboratory
Morris Good, Ryan Meyer
Pacific Northwest National Laboratory
Pradeep Ramuhalli
Oak Ridge National Laboratory
Luke Breon
Electric Power Research Institute

Dec. 2022

Idaho National Laboratory
Idaho Falls, Idaho 83415

http://www.inl.gov

Prepared for the
U.S. Department of Energy
Office of Nuclear Energy
Under DOE Idaho Operations Office
Contract DE-AC07-05ID14517

Page intentionally left blank

SUMMARY

This report summarizes an assessment conducted on the current state of structural health monitoring (SHM) technologies for supporting the deployment and monitoring of advanced reactor concepts.

Page intentionally left blank

CONTENTS

FIGURES

TABLES

ACRONYMS

ARD	advanced reactor developer
ASME	American Society of Mechanical Engineers
BPVC	Boiler and Pressure Vessel Code
EMAT	electromagnetic acoustic transducer
ISI	in-service inspections
LWR	light-water reactor
NDE	non-destructive examination
PZT	lead-zirconate-titanate
RIM	reliability and integrity management
SHM	structural health monitoring
SSCs	structures, systems, and components
TRL	technology readiness level

Page intentionally left blank

1. INTRODUCTION

To support missions extending beyond simple baseload electricity generation, advanced reactor types currently under consideration are expected to operate at higher temperatures than light-water reactors (LWRs). The combination of elevated temperature and different operating modes is expected to foster material aging mechanisms such as high-temperature creep and creep-fatigue. Methods of monitoring and detecting such mechanisms necessarily involve nondestructive evaluation (NDE) and/or structural health monitoring (SHM) techniques, with ultrasonic methods for NDE and SHM being of particular interest given their current widespread use in in-service inspections (ISIs). The present report summarizes a survey that was conducted on the recent literature in order to determine the current state of technology for high-temperature ultrasonics, for use as input to an assessment of sensor technology gaps in this application area.

Over the last several years, advanced non-light-water-cooled reactor concepts have moved ever closer to reality, with multiple options now nearing the design certification and licensing stages. The reactor designs being considered feature many of the concepts investigated within the Gen IV forum, and include liquid-metal, molten-salt, and gas coolants, as well as advanced fuel concepts (metal, ceramic, or liquid) that differ from existing commercial fuel designs.

One distinguishing factor of the advanced reactors currently under consideration is their operating temperature, which is considerably higher than that of LWRs. Coolant temperatures in excess of 300–400°C (and potentially approaching 1000°C) are normal for advanced reactors. These higher temperatures, when combined with the potential for fast neutron spectra, longer operating cycles, and highly corrosive coolants, could result in the need to monitor and detect structural material aging/degradation in various advanced reactor components. This report highlights the current state of technology for ultrasonic/acoustic sensors aimed at meeting this potential need for material aging/degradation monitoring.

2. BACKGROUND

Advanced non-light-water-cooled reactor concepts currently under development include liquid-metal-cooled reactors (typically sodium- or lead-cooled, including variants such as lead-bismuth eutectic), gas-cooled reactors (typically helium or CO_2), and molten-salt-cooled reactors. The molten-salt reactor concepts include both solid- and liquid-fueled concepts.

Reactor designs using these non-light-water coolant forms cover a range of power outputs, with micro- (<10 MWe), small modular (<300 MWe), and large (>300 MWe) reactors being proposed for various applications. Summaries of typical advanced reactor concepts (microreactor or small modular reactors) are available in numerous reports and papers (e.g., [1,2]), and it is worth noting that many of these concepts were demonstrated at different points in the nuclear era by employing research, test, and operational reactors, both in the U.S. and abroad.

Previous studies have documented the range of environmental conditions to which structures, systems, and components (SSCs) in these advanced reactors may be exposed [1]. These studies, which leveraged a range of publicly available information on designs, in addition to published information on previously operated reactors, indicate that the components and materials used in these reactor concepts are likely to see highly elevated temperatures (~350–900°C) during their operation. However, most advanced reactor concepts are lower pressure systems in comparison to the current LWR designs. Furthermore, many of the concepts expect to utilize non-traditional (non-baseload) operational concepts such as:

- Extended operating cycles (for power reactors) to increase the intervals between refueling outages. Cycle lengths of 10–30 years have been proposed for some concepts [3,4], in contrast to the current LWR fleet's typical operating cycle lengths of 18–24 months. On the other hand, certain microreactor concepts are expected to operate for very short durations, with extended shutdown intervals in between. This particular operating characteristic is tailored to emergency or backup power applications.
- Flexible operation to support grid stability in the presence of renewable generation sources. Traditionally, reactors in the U.S. have provided stable baseload power, though many LWR concepts are also capable of load-following operations. Indeed, reactors have been operated in load-following modes overseas, with the obtained operating experience subsequently being documented in various reports [5]. Non-baseload operation of advanced reactors is only expected to increase as use of renewable generation sources (solar and wind, in particular) on the grid continues to rise.
- Online refueling (as opposed to the current practice of refueling after the reactor undergoes cold shutdown).
- Potential for occasional relocation to different sites (pertains to microreactors).

Reactor designs and operational constraints ensure that the reactor and plant can be operated in a manner that does not allow for radioactivity release under normal and design-basis accident conditions. The designs focus on implementing strategies that do not rely on a single SSC to ensure safety; instead, multiple—and sometimes redundant—systems are utilized. While some safety-critical systems rely on active components (components that actuate or move), maintaining the integrity of passive components (e.g., piping and vessels) is also essential for maintaining safety via this defense-in-depth strategy.

The structural integrity of passive components is typically ensured through a combination of ISIs and maintenance activities. As discussed in [1], ISIs are required under 10 CFR 50.55(a) of the U.S. Code of Federal Regulations, along with NDE of structural components via techniques approved by the American Society of Mechanical Engineers (ASME) Boiler and Pressure Vessel Code (BPVC) and incorporated by reference in 10 CFR 50.55(a). In particular, Section XI of the BPVC includes inspection requirements and acceptance criteria for the LWR fleet [6]. However, BPVC requirements for advanced reactors remain a work in progress, with Section XI, Division 2 of the BPVC proposing a process for developing a reliability and integrity management (RIM) program for advanced reactors, similar the ISI programs for LWRs [1]. Such a program would need to identify degradation modes, reliability targets, etc., without specifying any particular strategies or targets for these quantities. As of mid-2022, the RIM program was being reviewed by the U.S. Nuclear Regulatory Commission, with draft guidance already having been made available [7].

Ultrasound, which uses high-frequency (at least 20 kHz, but typically in excess of 500 kHz for NDE applications) acoustic (in fluids) and elastic (in solids) waves, is sensitive to a number of material property changes, including changes in microstructure and the presence of cracking or other types of flaws such as porosity and inclusions. The measurement is also sensitive to temperature and material density changes. As a result, ultrasound has been used to characterize degradation, damage [8], and microstructures [9]; quantify and visualize structural changes [10]; and implement process control [11]. It is being actively investigated for post-irradiation examination of fuels [12] and is an excellent candidate for advanced reactor component SHM. However, acoustic/ultrasonic methods have seen limited applicability to the types of high-temperature environments typical of advanced reactors.

2.1 Structural Health Monitoring

When applied to advanced reactor designs, SHM can reduce the need for both intermittent inspections and onsite monitoring of reactor conditions. Specific nuclear energy program areas include advanced small modular reactors, LWR sustainability, advanced reactor technologies, and space/defense power systems. SHM crosscuts these to accomplish the following:

- Maintain safe, reliable, and efficient SSC operation, in accordance with the design intent [13]
- Reduce costs
- Improve the comprehensive life/aging management of SSCs
- Extend the operational lifetimes of power systems via retirement for cause.

One SHM concept is to permanently install sensors that provide feedback on material properties and SSC integrity, and to monitor degradation mechanisms (e.g., corrosion and cyclic stresses). Thus, innovation is needed to develop reliable sensors and instrumentation that can acquire measurements during reactor operation, robustly endure harsh environments for long durations (e.g., the operational life of the reactor system), and minimize system operation interference. Significant factors unique to each application include irradiation levels, temperature extremes and thermal cycles, and corrosion.

2.1.1 Acoustic Wave Modes for SHM

Three primary guided wave types are considered in SHM applications: surface waves (guided waves that are confined to within a few wavelengths of a free surface), plate waves (waves confined to thin structures such as plates and pipes), and bulk waves (only considered guided waves when confined to a waveguide). For the proposed testing configuration, any form of bulk wave can be represented as one of the plate modes.

2.1.1.1 Bulk Waves

Longitudinal Waves

Longitudinal waves represent the most basic wave mode used for SHM/NDE, as they can be transmitted through solids, gases, and liquids. In a longitudinal wave, the transmitted energy is in parallel with the particulate motion. They can be thought of as compression waves. Longitudinal waves are generally used for thickness measurements or flaw detection, and can be considered guided waves if confined within a waveguide (i.e., a thin rod or shell).

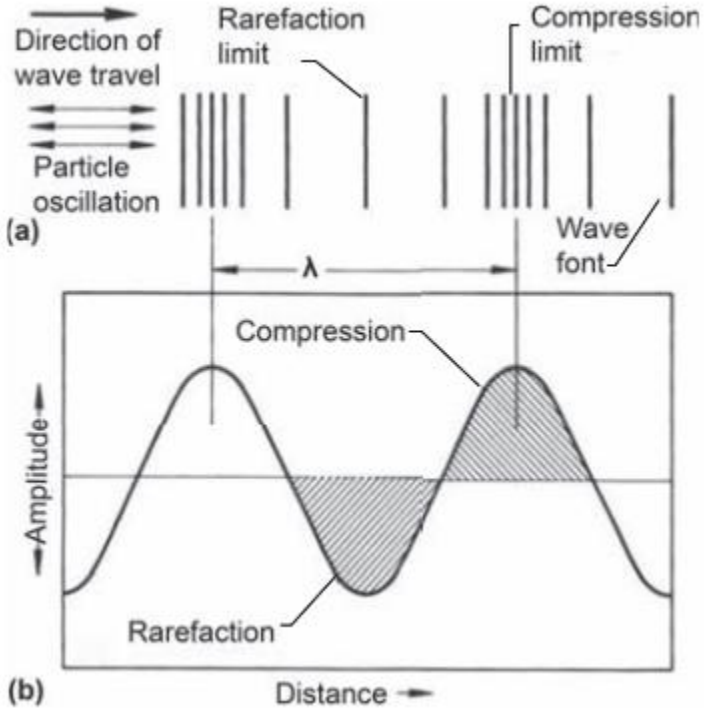

Figure 1. Graphical description of a longitudinal bulk wave (reproduced from [14]).

Shear waves

The second type of bulk wave is the transverse or shear wave. In this case, the direction of energy transfer is perpendicular to the direction of particle motion. Shear waves can be transmitted through solids and very viscous liquids. As with longitudinal waves, they can be considered guided waves if confined within a waveguide; in the case of a rod-like waveguide, they may be considered torsional or flexural waves.

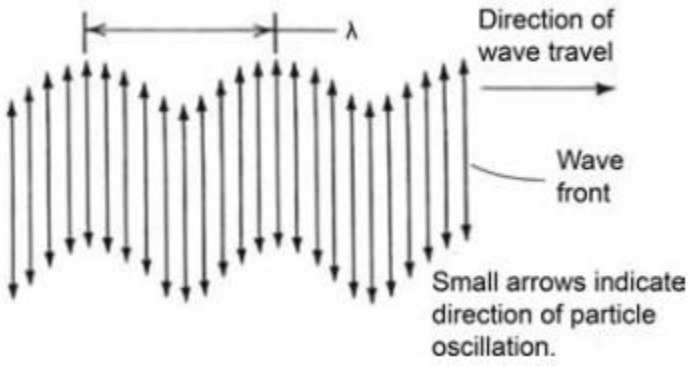

Figure 2. Graphical description of a longitudinal shear wave (reproduced from [14]).

2.1.1.2 Surface Waves

Some surface waves are considered promising for flaw detection in systems such as flow pipes and other structural components, as they are nondispersive, can operate at high frequencies (making them very sensitive to small surface-crossing flaws), and can follow surface contours (allowing access to hard-to-reach areas) [15].

Rayleigh Waves

Rayleigh waves (Figure 3) are surface-confined waves in which the direction of motion is normal to the free surface and perpendicular to the direction of energy transfer. Rayleigh waves are used in many sensors, as they are sensitive to small changes in the state of a substrate. As Rayleigh waves are confined to a wavelength-dependent surface depth, operation within a thin plate requires a minimum frequency of operation for it to still be considered a surface wave and not a plate wave. The depth is related to wavelength in that the depth is approximately half the wavelength. For a 0.11-in.-thick plate, this equates to a frequency of operation of ~1.6 MHz (using the shear wave velocity of zirconium to closely approximate the true wave velocity in the proposed sample). Most Rayleigh wave applications are targeted at several hundred MHz, with a practical minimum limit of ~3 MHz (a limitation on interdigitated electrode spacing while still carrying sufficient electric field strength to generate and sense the waves) [15,16]. As Rayleigh waves are attenuative, they are typically only used over relatively short distances (several cm in the presence of a viscous fluid) [17]. Rayleigh waves are considered Scholte waves when the free surface is in contact with a viscous fluid. Scholte waves are a “leaky” form of wave that loses energy to the fluid (in fact, the bulk of the acoustic energy is carried in the fluid) [15,17]. These waves are not appropriate for the proposed application.

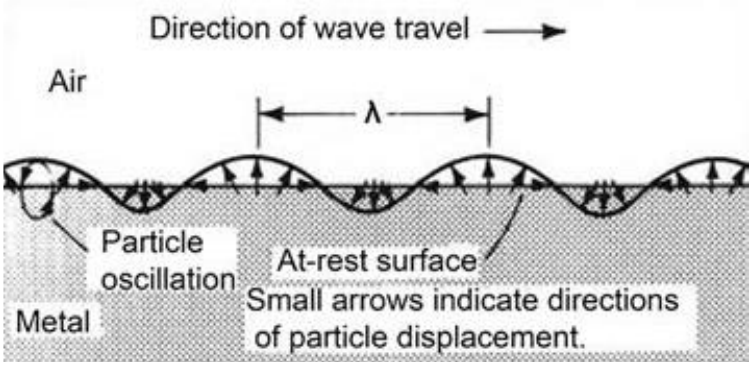

Figure 3. Graphical description of a Rayleigh surface wave, with the propagation direction being left to right (reproduced from [14]).

Love Waves

Love waves are surface waves in which the direction of motion is parallel to the free surface and perpendicular to the direction of energy propagation [15,16]. As with Rayleigh waves, love waves are attenuative and require a thin waveguiding layer to propagate. This is effectively a shear horizontal wave in the thin guiding layer, with acoustic coupling into the substrate layer. The waves are not sensitive to liquid layers in contact with the free surface, but energy does leak into the substrate. Love waves can be very sensitive to surface-breaking defects as well as to mass loading on the surface.

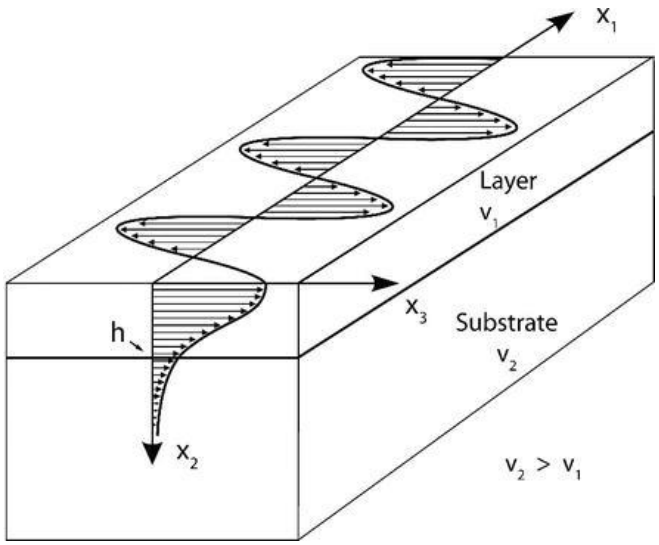

Figure 4. Graphical description of a love surface wave, with the propagation direction being from bottom-left to upper-right (reproduced from [18]).

2.1.1.3 Plate Waves

Whereas surface waves are confined to a small depth near a free surface, plate waves propagate over the entire thickness of a thin plate or thin-walled pipe [15,16]. These waves can be categorized into two basic types: Lamb waves and shear horizontal waves. Bulk wave analogues also exist for each of these types (longitudinal and shear.

Lamb Waves

Lamb wave modes can generally be thought of as being fundamentally similar to Rayleigh waves, though the wave energy is carried simultaneously on two sides of a plate (whereas the Rayleigh wave is

carried on one surface of a semi-infinite body). Lamb waves exist in two forms: symmetric and anti-symmetric (described in Figure 5, with energy travelling from left to right). The anti-symmetric Lamb wave is a flexural wave, while the symmetric mode is compressive. As both modes are out-of-plane relative to the surface of the plate, both wave modes are considered leaky.

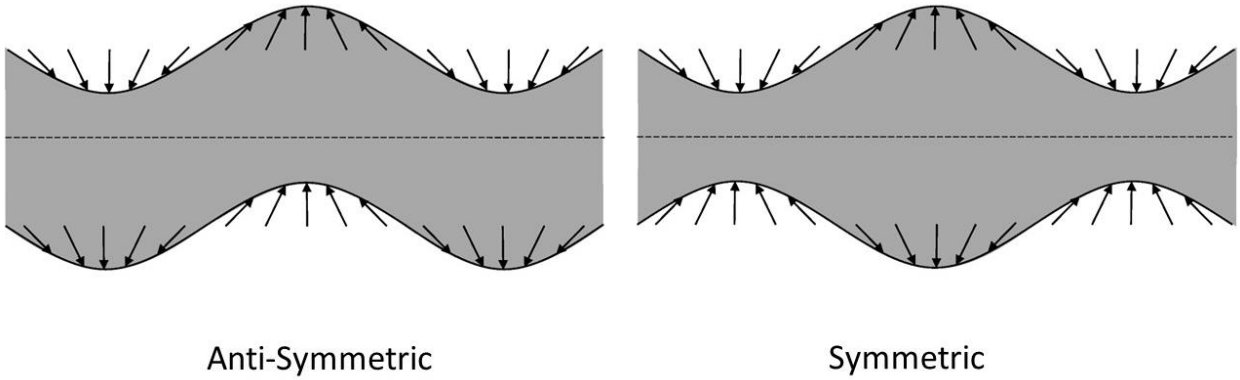

Figure 5. Graphical description of a Lamb plate wave, with the propagation direction being left to right (reproduced from [19]).

Shear Horizontal Waves

In the second type of plate wave, the shear horizontal wave, the particle motion and direction of energy travel are perpendicular to each other, as well as mutually perpendicular to the surface of the plate (i.e., the wave motion is in-plane). Shear horizontal waves are technically leaky, as some energy is lost at the edges (due to fluid damping) and on the surface (due to viscous effects), but these losses are very small compared to other leaky wave types.

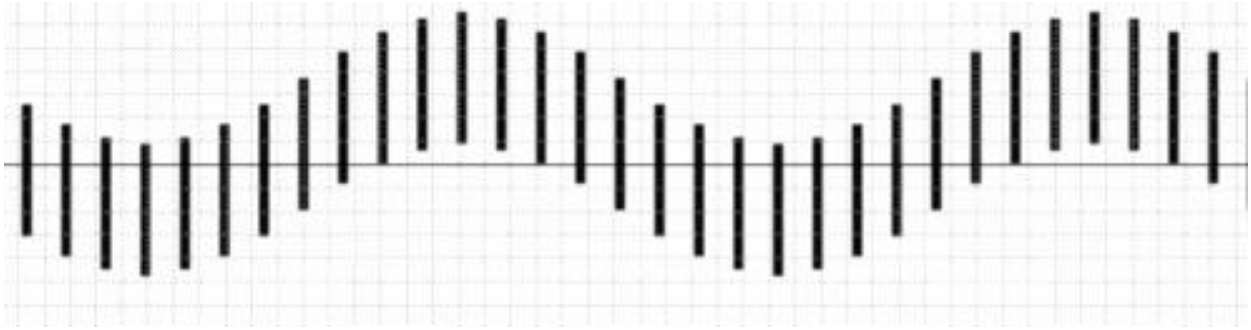

Figure 6. Graphical description of a shear wave, with the propagation direction being left to right. (reproduced from [14]).

2.1.2 Piezoelectric Technologies

The most commonly used ultrasonic transducer type is the piezoelectric crystal [20], which serves as both the generator and receiver of the acoustic pulse. Piezoelectric transducers typically consist of either a single crystal or a ceramic compound chip wafer that will contract and expand, creating a corresponding acoustic wave when excited by an oscillating external electric field. Conversely, an electric field is generated when the crystal is exposed to external stress. This wave may be coupled to an external sample, or the piezoelectric crystal may be used as an intrinsic sensor. The wave modes that are generated and detected are dependent on how the crystal is cut and poled, the design of the electrodes, and the manner of coupling to a sample. Several piezoelectric materials have been used and tested in radiation environments [20], and a few have shown the necessary radiation tolerance required for the proposed application [21].

Newer materials such as scandium-doped aluminum nitride (currently only used as a thin film) [22] show great promise but have yet to be tested in harsh enough conditions to instill confidence in their long-term performance. In general, piezoelectric materials are either inherently piezoelectric due to their crystal structure, or must be poled via exposure to a strong electric field. Naturally, piezoelectric materials are more radiation tolerant but tend to have lower electro-acoustic efficiency.

Ultrasonic methods have seen limited application in environments typical of proposed advanced reactor designs. A major factor in this is the limited survivability of conventionally available ultrasonic sensors, such as the commonly used lead-zirconate-titanate (PZT) piezoelectric sensor material. PZT's applicability is generally limited to environments featuring temperatures of less than 300°C, though the temperature limit may be increased with external cooling options. While other piezoelectric options do exist (e.g., bismuth titanate, aluminum nitride, and lead metaniobate), and have been the subject of various experiments [21,23-25], the sensitivity of the sensor material may be low at high temperatures.

Since piezoelectric sensors are currently the predominant method of ultrasonic NDE, understanding the various mechanisms by which they can fail may provide insights into the selection of different sensor materials and the design of new sensors. Piezoelectric materials such as PZT, barium titanate, and sodium bismuth titanate are a type of ferroelectric, and the application of an electrical voltage results in the development of mechanical strain. Such materials are known to be susceptible to fatigue, due to electrical loading (degradation under service conditions) and time-dependent aging (degradation under external equilibrium conditions)—even in the absence of mechanical or electrical loading [26]. Aging and degradation are commonly attributed to the formation of vacancies (microstructural changes) in the material, and these impact the ability to switch ferroelectric domains under an applied electric field, though these are also attributed to other mechanisms [27-29]. Operation at elevated temperature can increase degradation due to fatigue and aging [29], while operation in the presence of neutron radiation can cause amorphization [26], loss of piezoelectricity as a result of the transmutation of constituent elements, or depoling due to localized thermal spikes caused by fast neutron interactions [21]. Factors such as loading frequency, pre-loading of the piezoelectric, microstructural defects, and material composition (including the presence of impurities) affect the rate at which degradation accumulates in these materials. Interestingly, there is evidence of some doped piezoelectrics' properties being recovered (de-aging) under electric field cycling [28]. In addition to the impact on piezoelectric sensitivity, aging and fatigue degradation also affect the ability to perform accelerated aging studies at elevated temperatures. However, online signal monitoring may provide insights into sensor survivability and drift, and enable calibration of the measured response for specific operating environments.

2.1.2.1 State of Technology for Advanced Reactor Applications

The properties that are the most relevant to measurements in radiation environments include maximum operating temperature, sensitivity, and resistance to radiation damage. Material selection involves trade-offs regarding these properties. For many piezoelectric materials, the Curie temperature, T_c (from which the maximum operating temperature can be inferred), and electromechanical coupling coefficient are known. Data on the radiation resistance of nearly all materials are incomplete, and materials are rarely tested under the same conditions, making comparisons hard or even impossible. Table 1 lists the piezoelectric materials considered for irradiation applications.

Table 1. Piezoelectric material summary.

Material	Transition Temperature (°C)	Transition Type	Problematic Atomic Species (ENDF)	d33
PZT	365	Curie temperature	Pb	375
Quartz	550	Curie temperature	NA	2
Lead meta-niobate	400	Curie temperature	Pb	85
AlN [20, 21, 30, 31, 32, 33, 34]	2200	melt	NA	0.2
$LiNbO_3$ [35, 36]	1050–1210	Curie temperature	Li-6	0.46
$GaPO_4$ [32, 37]	970	α–β	NA	0.16
Bi_3TiNbO_9 [20, 21, 33, 37, 38]	909	Curie temperature	NA	18
$[ReCa_4O(BO_3)_3]$ [37]	1500	melt	Boron	0.06–0.31
ZnO [20, 21, 32, 33, 39]	>1500	melt	NA	0.4
$La_2Ga_5SiO_{14}$ [32, 40]	1470	melt	NA	??

Several of these materials have undergone gamma or neutron irradiation testing, demonstrating widely varying levels of radiation tolerance. PZT is the piezoelectric material most commonly used today, due to its extremely high electromechanical efficiency (characterized by the d33 term). However, it has both a low Curie temperature (at which point it loses its piezoelectric properties) and very poor radiation tolerance. PZT is a material that must be poled (i.e., subjected to a high external electric field) to become piezoelectric. Poling induces permanent deformation of the material's crystal lattice, resulting in the creation of an electric dipole. Under irradiation, this poling can be lost through various mechanisms. First, the Curie temperature may be exceeded, either through the environmental temperature exceeding T_c, or through radiation-induced heating, even including individual thermal spikes caused by neutron impacts. Poling can also be lost through crystal amorphization due to fast neutron damage. In general, piezoelectric materials that must be poled have poor irradiation tolerance. Other materials such as aluminum nitride are naturally piezoelectric thanks to their crystal structure. These materials tend to have much lower d33 values but much higher radiation tolerance. Aluminum nitride, bismuth titanate niobate, and zinc oxide were tested in the Massachusetts Institute of Technology Research Reactor [21,33] to a fast neutron fluence of 8.8×10^{20} n/cm^2. Of these, only aluminum nitride exhibited sufficient performance to be considered for long-term in-core applications. Lithium niobate is thought to be radiation tolerant due to its crystal structure, and its ultrasonic properties are superior to those of aluminum nitride, but it has not been tested to high fluence levels, and the presence of Li-6 is likely to slow the loss of piezoelectricity under thermal neutron flux, due to transmutation of the lithium to helium. Only aluminum nitride has proven radiation tolerant enough to be considered, but it has very poor piezoelectric properties and is not an ideal candidate for any extrinsic application.

2.1.3 Magnetostrictive Technologies

Magnetostriction is a material property via which a change in dimensions or strain occurs when the material is subjected to an applied magnetic field. The inverse, or Villari, effect is a change in magnetic susceptibility when the material is subjected to stress [41]. A time-varying magnetic field applied to a magnetostrictive material can thus generate an acoustic wave, and acoustic waves can be detected by the

inverse process. Significant issues are the maximum working temperature of key materials and the effective and stable ultrasonic coupling between the magnetostrictive material and the material/part of interest. An important material parameter is the Curie temperature, which is a temperature maximum above which ferromagnetic behavior ceases for the material. The maximum service temperature is obviously lower than the Curie temperature, but is a subjective value and is often not listed.

Selected magnetostriction applications include sensors for ultrasonic inspection, material degradation, temperature, and part position. A driving factor is that some magnetostrictive materials can withstand harsh environments involving high irradiation levels, high temperatures, corrosion, etc.

As with piezoelectrics, the important properties of magnetostrictive materials are maximum operating temperature (also related to a Curie temperature), sensitivity (typically related to the saturation magnetostriction), and resistance to radiation damage. Magnetostrictive materials are generally either pure metals or alloys, with the alloys having much higher magnetostriction—often at the cost of a lower T_c. Table 2 lists the magnetostrictive materials considered for in-core use.

Table 2. Magnetostrictive material summary.

Magnetostrictive Material	Trade Name	Curie Temp. (°C)	Problematic Species	Saturation Magnetostriction (μm/m)
Ni [41]	Nickel	354	NA	~50
Fe [41]	Iron	770	NA	~20
Co [41]	Cobalt	1120	Co	~60
95Fe-5Cr, 92Fe-8Mn [20, 21, 33]	Arnokrome	770	NA	~40
50Fe-50Co [41, 42, 43]	FeCo or ferrous cobalt	938	Co	~100
49Fe-49Co-2V [20, 21, 33]	Remendur	950	Co	~100
30Fe-70Co [44]	—	>730	Co	~70
87Fe-13Ga [20, 21, 33]	Galfenol	700	NA	~300
82Fe-13.5Ga-4.5Al [44]	—	>730	Na	~400
99.4(83Fe-17Ga)-0.6B [44]	—	>730	Boron	~100
0.3Tb-1.92Fe-0.7Dy [41]	Terfenol-D	380	NA	~2,000
81Fe-3.5Si-13.5B-2C [41]	Metglas 2605SC	370	Boron	~50

Galfenol and Terfenol-D are so-called “giant” magnetostrictive materials, with magnetostriction in the hundreds of microstrains. This makes them very appealing for sensing and actuation applications. The very low Curie temperature of Terfenol-D, coupled with its extreme brittleness and difficulty to fabricate, make it less promising for in-core applications. Most other available alloys with high magnetostriction contain cobalt, which may be a concern due to the fact that activation of the element turns it into a strong gamma emitter. Very few magnetostrictive materials have been tested in an in-core environment, but several (Remendur, Galfenol, and two Arnokrome alloys) were included in the aforementioned

Massachusetts Institute of Technology Research Reactor irradiation test [20,21,33]. The Galfenol and Remendur samples were interrogated in real-time, while the Arnokrome samples were "drop ins" that were examined during post-irradiation testing. All the tested magnetostrictive samples retained full magnetostriction after the test, though the real-time-interrogated samples did show degradation during the test (thought to be primarily due to thermal and mechanical effects). It has been theorized that the high radiation resistance of magnetostrictive materials is driven by the fact that the induced strain is caused by the alignment of magnetic domains within the material. These domains may become pinned at grain boundaries, broken up, and made smaller, but still retain the ability to align in the presence of an external magnetic field.

Just as most piezoelectrics must be poled to enhance their properties, magnetostrictives must typically be biased by an external magnetic field. Thus, either a permanent magnet or a DC magnetic field coil must be included in the magnetostrictive sensor. The properties of high-temperature magnets are summarized in Table 3.

Table 3. Magnet material summary.

Magnet Material	Curie Temp. (°C)	Problematic Species	Comments
Ferrite	770	NA	Various types based on dopants, relatively low magnetic strength, better used for magnetic circuit parts
Alnico	860	Co	Several types based on Al, Ni, Co alloy amounts and dopants; low magnetic strength; high T_c
Nd-Fe-B	370	B, Nd	Very low Tc, very high magnetic strength
Sm-Co	850	Co	Several types based on Sm, Co amounts; high magnetic strength; high T_c

2.1.3.1 Magnetostrivctive Temperature Limits and the Presence of Cobalt

A typical magnetostrictive inspection transducer consists of a magnetostrictive material, magnetizing coil, method of creating a magnetic bias, material to complete the magnetic circuit, and means of coupling ultrasonic waves between the magnetostrictive material and the material or part of interest. Higher temperature applications typically substitute materials with higher temperature specifications. As temperatures continue to increase, material and transducer designs eventually require alternative approaches to achieve operation.

Many magnetostrictive materials and permanent magnets contain Co, especially those with a high Curie temperature (Table 2 and Table 3). Thus, a key issue is whether such materials should be excluded due to concerns about the production of Co-60 during irradiation.

Three magnetostrictive materials that do not contain Co and have a relatively high Curie temperature are 82Fe-13.5Ga-4.5Al, 99.4(83Fe-17Ga)-0.6B, and Fe with Curie temperatures of >730, >730, and 770°C, respectively. In contrast, the Curie temperature of Co is 1120°C.

Neodymium magnets and ferrite are permanent magnets that do not contain Co, and feature maximum Curie temperatures of 370 and 771°C, respectively. In contrast, samarium-cobalt and alnico (an alloy primarily of Al, Ni, and Co) permanent magnets have maximum Curie temperatures of 850 and 860°C, respectively. Grain-oriented Si Fe (roughly 97Fe-3Si) may be used as an electromagnet core, and it has a Curie temperature of 740°C; thus, from a temperature perspective, there seems little advantage in using an electromagnet if ferrite is successfully being used as a permanent magnet.

Therefore, if materials with Co are excluded from the magnetostrictive sensor, the Curie temperature limit is 770°C. Use of an electromagnet to replace the permanent magnet could be useful if the ferrite

magnets are too weak, but this would decrease the Curie temperature limit to 740°C. If materials with Co are permitted, the combination of Co based magnetostrictives and alnico permanent magnets would afford a Curie temperature limit of 860°C. If a permanent magnetic bias could be preset and sustained in the Co material, the permanent magnet would no longer be needed, and the Curie temperature limit would be 1120°C. A case in which such a magnetic bias was preset and sustained in two magnetostrictive materials during an irradiation test is discussed later in this report.

Assuming high-irradiation environments and the exclusion of Co from use, development of magnetostrictive materials, permanent magnets, and electromagnet core materials with Curie temperatures ranging from 770°C to well over 1000°C is needed. If successful, SHM sensors based on magnetostrictive technologies could potentially provide SHM of the broad set of advanced reactor types.

2.1.4 Electromagnetic Acoustic Transducers

Electromagnetic acoustic transducers (EMATs) work in a similar manner as magnetostrictives, except that they do not require a special material to couple with the field coil. Instead, EMATs use an oscillating magnetic field to create eddy currents in conductive materials. This leads to the generation of Lorentz forces, which in turn generate acoustic waves. Waves are detected via the inverse process. As with magnetostrictives, the wave modes generated through EMATs can, to an extent, be controlled by tailoring the operational frequency and the polarity of the coil and required biasing magnet. Signals generated by EMATs are much weaker than those generated using piezoelectric or magnetostrictive methods, and thus require significant amplification, resulting in high levels of signal noise. EMATs are capable of high-temperature operation (limited by the Curie temperatures of the biasing magnet, coil materials, and natural acoustic attenuation of the interrogated sample), and have been demonstrated to ~900°C for short durations [45]. As EMATs are comprised of a magnet (or DC coil) and an AC coil, radiation tolerance is not an issue.

2.1.5 Lasers/Others

Outside the nuclear industry, laser-based methods are gaining popularity either as a standalone solution or as part of a hybrid setup (i.e., using a laser to generate signals, and a piezoelectric transducer for reception) [46-48]. Laser-based systems use a high-energy laser to create a short thermal pulse at the sample surface. This generates a broadband signal comprised of any wave modes that the sample can support. The acoustic signals can then be detected by using either another light-based method (laser vibrometer, Fabry-Perot interferometer, etc.) or by using a traditional transducer. The reverse setup can also be used (traditional transducer to apply energy, and an optical method for detection). The applied wave modes can, to an extent, be controlled using a shaped receptor (i.e., a wedge) attached to the sample as a target. The multimodal acoustic waves are generated in the wedge and primarily converted into another form (e.g., Lamb waves) within the sample. The lasers can be fiber-coupled to enable remote delivery and detection.

Laser ultrasound applications require either a line of sight to the target or fiber delivery. Line of sight is generally not possible, as most reactor components of interest will be heavily insulated. Optical fibers are among the most researched sensor technologies for in-core applications, since their advantages are numerous (high fidelity, distributed measurements, immunity to electromagnetic noise, etc.). The two most studied types of fiber are silica based and sapphire based. It has been known for decades that silica fibers will darken (i.e., lose transmissibility) under gamma and neutron irradiation. This darkening is strongly dependent on the light wavelength and the chemical makeup of the fiber. In the communication industry, germanium-doped fibers are the norm, as they have extremely low losses and can carry signals across vast distances. However, germanium-doped fibers are also the most susceptible to darkening. Recent studies indicate that a pure silica fiber with a fluorine-doped cladding will darken to an extent, but that the darkening will saturate [49]. A second radiation effect on silica fibers is compaction. The fiber shrinks over time, changing both its geometry and calibration (for intrinsic sensors). The compaction

effect has not been shown to saturate, and will seemingly continue for the duration of an irradiation, possibly leading to catastrophic failure of the fiber, which becomes brittle as it compacts.

2.1.6 Commercial Availability

Table 4 summarizes the studies conducted on four different types of acoustic sensors: piezoelectric sensors, EMATs, magnetostrictive sensors, and laser ultrasonics. The references in these four types each correspond to a temperature range and technology readiness level (TRL). The TRL of each reference is not strictly evaluated. But in general, if a transducer or system is only studied in a laboratory environment, we define it as TRL 1–3. If the transducer or system has been validated in an industrial application, it is defined as TRL 4–6, whereas a TRL of >6 reflects successful commercialization of the transducer or system. The temperatures are grouped into four ranges: 50–250, 250–500, 500–1000, and >1000°C.

For the piezoelectric sensors, the temperatures in these studies range from 200 to 1600°C. At a very high temperature (>1000°C), Prasad et al. [50] employed an Al_2O_3 buffer rod surrounded by a circulating cooling system, and Wei et al. [51] used a similar design. Periyannan et al. [52] developed a bent rod as the waveguide for high-temperature measurements. Most of these studies here have a TRL of 1–3, which were only performed in a lab environment. The study by Cheong et al. [53] has a TRL of 4–6, since their ultrasonic thickness monitoring system was tested in a flow-accelerated corrosion-proof test facility. A high-temperature ultrasonic transducer injected an ultrasonic wave into the pipe via a short buffer rod and a gold plate for pipe wall thickness monitoring.

For EMATs, the maximum temperature in these studies was around 900°C. Burrows et al. [45] developed a water-cooled EMAT shear wave sensor for measuring the thickness of stainless and low carbon steels. The EMAT in the system was used as the receiver, while a Nd:YAG laser served as the transmitter for injecting the ultrasonic wave. In the table, two EMAT studies for TRL of 4–6 were listed. Kogia et al. [54] manufactured a prototype of an oil-cooled EMAT sensor for temperature measurements at up to 500°C, and Baillie et al. [55] implemented a laser-EMAT system for defect detection on an 800°C pilot-scale rolling mill in a steel plant.

In recent studies, the magnetostrictive sensor had a maximum operating temperature of 530°C in table 4. (The high-temperature magnetostrictive sensor is still in the early stages of being studied, and thus the results are not listed here.) Several magnetostrictive sensor studies with TRL of 4–6 were also listed. Vinogradov et al. [43] developed a magnetostrictive transducer system for pipe SHM, using a guided wave at 200°C. Under neutron irradiation in a nuclear reactor, Reinhardt et al. [56] tested two magnetostrictive sensors, one fabricated from Remendur and one from Galfenol, at a temperature of 420°C.

In recent years, laser ultrasonics has been widely used for high-temperature sensing, as it does not require direct contact with hot surfaces for ultrasonic wave transmission/reception. Several studies of using laser ultrasonics are listed in table 4 for high-temperature measurements from 200°C to 1400°C. Matsumoto et al. [47] used a laser interferometer to measure the elastic properties of ceramic at 1400°C. Quintero et al. [46] utilized laser ultrasonics to inspect the SiC/SiC composite with C-scan to locate impact defects and cracks at room temperature to 1250°C. Yu et al. [48] combined laser ultrasonic excitation and fiber-optic Bragg gratings for defect detection on a ceramic plate at 1000°C.

Commercial acoustic/ultrasonic transducers for high-temperature applications also exist. Such transducers and systems are summarized below.

1. Commercial high-temperature piezoelectric sensors:
    - Piezo Technologies (up to 260°C)
    - Olympus (up to 500°C)
    - HotSense (up to 550°C)

- GE (transducer, delay line, wedge, couplant, ~200°C)
- Phoenix ISL (120°C)
- Physical Acoustic (acoustic emission sensor, 540°C).

2. Commercial high-temperature EMATs:
    - Olympus (up to 60°C),
    - Innerspec (200°C for an unlimited time, 600°C for 5 seconds)
    - Sonemat (up to 550°C)
    - Simpleoilfield (up to 700°C).

3. Laser ultrasonics:
    - Quantel and Brilliant Ultra: Nd:YAG pulse laser
    - Polytec: fiber-guided laser OFV-551
    - Nd:YAG laser from TEEM Photonics.

Table 4. Elevated/high-temperature acoustic sensor technologies covered in the literature.

		Piezoelectric Sensor			EMAT			Magnetostrictive Sensor			Laser Ultrasonics		
	TRL	1–3	4–6	>6	1–3	4–6	>6	1–3	4-6	>6	1–3	4–6	>6
Temperature range	50–250°C	[57], 216°C [58], 200°C [59], 55°C [60], 220°C [61], 200°C	[53], 200°C		[66], 250°C			[73], 200°C; [74], 200°C	[76], 200°C; [77], 200°C		[78], 200°C	[85], 110°C	
	250–500°C	[31], 450°C			[67], 250°C [68], 450°C [69], 500°C	[67], 500°C		[44], 500°C	[56], 420°C		[79], 300°C [80], 350°C		
	500–1000°C	[62], 730°C [63], 600°C [64], 700–800°C			[70], 600C° [45], 900°C [71], 700°C [72], 600°C	[55], 700°C		[75], 530°C			[81], 1000°C [82], 800°C [83], 950°C [84], 750°C		
	>1000°C	[65], 1400°C [50], 1400°C [51], 1600°C [52], 1200°C									[47], >1400°C [46], 1250°C [48], 1000°C		

2.2 Advanced Reactor Technologies

Conversations with advanced reactor developers (ARDs) have revealed that, though most of the conceptual designs are well developed, the planning for instrumentation and monitoring technologies is much less advanced. To the degree possible, standard nuclear instrumentation will be used (e.g., thermocouples and ex-vessel radiation monitors). Newer technologies will be needed for conditions in which standard instruments cannot operate and there is strong interest in online monitoring of both process parameters and reactor conditions (SHM), but those technology gaps have yet to be addressed by any of the contacted ARDs. Furthermore, a driving force behind industry adoption of new technologies and monitoring strategies is regulator requirements. According to conversations with ARDs, they have had little engagement with industry regulators on the topics of instrumentation and health monitoring needs. Given the state of planning and regulatory engagement that has been reached at this point, only a general assessment can be made as to industry needs regarding SHM. In general, the primary ARDs' technologies and corresponding expected temperatures are listed in Table 5.

Table 5. Characteristics of selected advanced fission reactors.

Reactor Type	Neutron Spectrum	Coolant	Outlet Temperature (°C)
Light-Water Small Modular Reactor	Thermal	Water	300–330
Lead Fast Reactor	Fast	Liquid Lead	480–570
Sodium-Cooled Fast Reactor	Fast	Liquid Sodium	500–550
Supercritical-Water-Cooled Reactor	Thermal/Fast	Water	510–625
Molten-Salt Reactor	Thermal/Fast	Molten Salts	700–800
Gas Fast Reactor	Fast	Helium	850
High-Temperature Gas Reactor / Very-High-Temperature Reactor	Thermal	Helium	700–1000

3. TECHNOLOGY GAPS

Given the lack of information on specific ARD needs, the following sections describe generalized technology gaps and the research needed to address them.

3.1 SHM Technology Gaps and Research Needs

3.1.1 Material Needs

These studies indicate a potential set of technical gaps associated with high-temperature ultrasonic sensors, including the potential need for high-temperature piezoelectrics that afford greater sensitivity than the materials tested to date, the need to develop techniques for accelerated laboratory testing of sensor materials in order to quantify degradation rates under typical advanced reactor conditions, and the need to develop techniques for calibration and compensating for degradation. Of particular interest is the need to test and evaluate potential commercially available sensors and sensor materials in order to determine their applicability to SHM and NDE for advanced reactors. In general, currently available sensors and systems must be tested for use in advanced reactor conditions, and new materials must be identified/developed for conditions under which no commercial sensor is viable.

3.1.2 Algorithm/Signal Processing Development

Since one aim of advanced reactor SHM applications is to enable remote/automated control, new SHM system control and data automation processing methods must be developed. Currently, SHM is conducted manually via an as-needed or as-scheduled process in which degradation/damage is determined by an inspector/technician. This process may be streamlined and automated by using permanently installed SHM sensors and advanced characterization algorithms, likely incorporating digital twins.

3.1.3 Ultrasonic Coupling between Sensors and Materials/Parts

Multiple ultrasonic coupling cases exist that depend on the characteristics of the localized area of the part on which the sensor is placed. Three cases of ultrasonic coupling were examined, with examples provided for each. These three cases are as follows:

- The part is directly interrogated, and coupling is not an issue—as may be the case with EMAT or laser ultrasound.
- An active material is intimately joined to a localized region of a part, and coupling is not an issue for a robust joining process—as may be the case with a magnetostrictive material brazed/welded/cold-sprayed onto a part.
- An active material is external to the part and requires coupling between the sensor and the part of interest—as may be the case with piezoelectric transducers.

EMATs can couple electromagnetically with any conductive material, so coupling is not generally an issue. Laser ultrasound requires line of sight and may not be appropriate for application to thermally insulated parts. If line of sight can be achieved, potential issues such as ablation of the interrogated material must be studied. For magnetostrictive materials, joining to a metallic component may be as simple as welding or brazing a magnetostrictive patch to the part to be interrogated. These methods of coupling may cause changes to the substrate, which must be studied. In the case of piezoeletrics, coupling to metallic parts is more complex, as acoustic impedances should be matched for optimal energy transmission. Permanent adhesion of a piezoelectric transducer is being studied by the Electric Power Research Institute through a Nuclear-Science-User-Facilities-funded irradiation experiment that aims to study several different ceramic cements in terms of both longevity and sound transmission. The results of this experiment have not been published as of this writing, but given the small sample size of this test, additional testing is warranted.

3.2 Regulatory Requirements

A RIM program is currently being developed by the ASME BPVC Section IX, Division 2 to generally address the aging of nuclear facilities. Advanced reactors are one of the nuclear facility subsets that the RIM program is intended to cover. Currently operating LWRs fall under the scope of Section XI, Division 1 of the ASME BPVC. The reason for developing the RIM program is to obtain a code that is technology neutral and can be applied to a variety of nuclear facility types. Its development was initiated by South Africa's interest in pebble-bed modular reactors in the early 2000s, and can be viewed as an attempt to incorporate lessons learned through the implementation of Section XI, Division 1—particularly with respect to the adoption of probabilistic risk assessment to prioritize those SSCs that should be included within the scope of an aging management program. A core philosophy behind RIM is that users must quantitatively define the reliability targets for SSCs within scope, and that users will have flexibility in selecting strategies to meet those reliability targets. These RIM strategies may be based on design, operation, and/or inspection and monitoring. The limited opportunities to apply RIM to date have caused its state of development to remain at a high-level, with significant additional detail desired in order to provide useful guidance to technology vendors.

3.3 Workshop

Based on conversations with ARDs, a primary focus of near-term efforts should be the fostering of engagement between ARDs and regulatory bodies such as the Nuclear Regulatory Commission and the Nuclear Energy Institute. A 1- or 2-day workshop was proposed for enabling ARDs, regulators, and SHM researchers to discuss needs, available technologies, and necessary technological advancements.

4. CONCLUSIONS

The objectives of advanced fission reactor SHM include the following:

- Maintain safe, reliable, and efficient SSC operation, in accordance with the design intent
- Reduce costs
- Improve the comprehensive life/aging management for SSCs
- Extend the operational lifetimes of power systems via retirement for cause.

The advanced reactor types currently under consideration are expected to operate at higher temperatures than LWRs, and support missions extending beyond simple baseload electricity generation. The combination of elevated temperature and different operating modes is expected to foster material aging mechanisms such as high-temperature creep and creep-fatigue. Methods of monitoring and detecting such mechanisms necessarily involve NDE and/or SHM techniques, with ultrasonic methods being an ideal candidate given their widespread use for NDE. This document summarized the state of technology for high-temperature ultrasonics, as part of an assessment of technology gaps and needed research. To date, the great majority of sensor development activities address elevated temperatures and radiation tolerance, and more work is needed in both areas. Few data exist regarding the corrosion effects of advanced coolants on sensor materials and couplants. Of high importance is the need for ARDs and regulatory bodies to engage and define what level of SHM is needed to enable autonomous or semi-autonomous reactor control.

5. REFERENCES

1. Meyer, R. M., et al. 2013. "Technical Needs for Prototypic Prognostic Technique Demonstration for Advanced Small Modular Reactor Passive Components." Richland, WA: Pacific Northwest National Laboratory. https://www.pnnl.gov/publications/technical-needs-prototypic-prognostic-technique-demonstration-advanced-small-modular.
2. Testoni, R., A. Bersano, S. Segantin, "Review of nuclear microreactors: Status, potentialities and challenges" Progress in Nuclear Energy, 2021. **138**: 103822.
3. Smith, C. F., et al., "SSTAR: The US lead-cooled fast reactor (LFR)." Journal of Nuclear Materials, 2008. **376**(3): 255-259.
4. Tsuboi, Y., et al., "Design of the 4S Reactor." Nuclear Technology, 2012. **178**(2): 201-217.
5. IAEA, "Non-baseload Operation in Nuclear Power Plants: Load Following and Frequency Control Modes of Flexible Operation." IAEA Nuclear Energy Series No. NP-T-3.23, IAEA, Vienna (2018).
6. Doctor, S. R., "Nuclear Power Plant NDE Challenges — Past, Present, and Future." AIP Conference Proceedings, 2007. **894**(1): 17-31.
7. U.S. Nuclear Regulatory Commission, 2021. "Acceptability of ASME Code, Section XI, Division 2, "Requirements for Reliability and Integrity Management (RIM) Programs for Nuclear Power Plants, For Non-Light Water Reactors, in Proposed new Regulatory Guide." **1,** 246. https://www.federalregister.gov/documents/2021/09/30/2021-21295/acceptability-of-asme-code-section-xi-division-2-requirements-for-reliability-and-integrity.
8. Ensminger, D., L. J. Bond, "Ultrasonics: Fundamentals, Technologies, and Applications." 3rd ed. 2012: CRC Press.
9. Ramuhalli, P., et al. "In-situ Characterization of Cast Stainless Steel Microstructures. in 9th International Conference on NDE in Relation to Structural Integrity for Nuclear and Pressurized Components," Seattle, Washington: May 22-24, 2012. Brussels, Belgium: Joint Research Centre, European Commission.
10. Larche, M. R., et al. 2015. "Progress in the Development and Demonstration of a 2D-Matrix Phased Array Ultrasonic Probe for Under-Sodium Viewing," in *Review of Progress in Quantitative Nondestructive Evaluation (QNDE 2015)*.
11. Lynnworth, L. C., "Ultrasonic Measurements for Process Control: Theory, Techniques, Applications." Elsevier Science: 2013.
12. Baron, D., D. Laux, G. Despaux, "Mechanical characterisation of irradiated fuel materials with local ultrasonic methods. in Pellet-clad Interaction in Water Reactor Fuels." Aix-en-Provence (France): Organisation for Economic Co-Operation and Development - Nuclear Energy Agency, 75 - Paris (France): 2004.
13. Rao, G. N. 2014. "In-service Inspection and Structural Health Monitoring for Safe and Reliable Operation of NPPs." *Procedia Engineering*, vol. 86 (2014), 476–485. ISSN 1877-7058. https://doi.org/10.1016/j.proeng.2014.11.061.
14. Bond, L. 2018. "Fundamentals of Ultrasonic Inspection," in ASM Handbook, Volume 17, *Nondestructive Evaluation of Materials*, ed by: Aquil Ahmad and Leonard J. Bond, 155–168. ASM International. https://doi.org/10.31399/asm.hb.v17.a0006470.
15. Rose, J. L. 2014. *Ultrasonic Guided Waves in Solid Media*. Cambridge, UK: Cambridge University Press. https://doi.org/10.1017/CBO9781107273610.

16. Mandal, D., S. Banerjee. 2022. “Surface Acoustic Wave (SAW) Sensors: Physics, Materials, and Applications.” Sensors 22(3): 820. https://doi.org/10.3390/s22030820.

17. Vanneste J., O. Bühler. 2011. “Streaming by leaky surface acoustic waves.” *Proceedings of the Royal Society A: Mathematical, Physical and Engineering Sciences*, **467**(2130): 1779–1800. http://doi.org/10.1098/rspa.2010.0457.

18. Kiełczyński, P. 2018. “Properties and Applications of Love Surface Waves in Seismology and Biosensors.” *In Surface Waves - New Trends and Developments*, ed by: Farzad Ebrahimi, IntechOpen. https://doi.org/10.5772/intechopen.75479.

19. Vázquez, S., J. Gosálbez, I. Bosch, A. Carrión, C. Gallardo, J. Payá. 2019. “Comparative Study of Coupling Techniques in Lamb Wave Testing of Metallic and Cementitious Plates.” *Sensors*, 2019: **19**(19): 4068. https://www.mdpi.com/1424-8220/19/19/4068.

20. Daw, J. E., J. L. Rempe, B. R. Tittmann, B. Reinhardt, P. Ramuhalli, R. Montgomery, H. T. Chien. 2012. “NEET In-Pile Ultrasonic Sensor Enablement-FY 2012 Status Report.” INL/EXT-12-27233, Idaho National Laboratory. https://doi.org/10.2172/1058076.

21. Daw, J., J. Rempe, J. Palmer, P. Ramuhalli, P. Keller, R. Montgomery, H.T. Chien, B. Tittmann, B. Reinhardt. 2014. “NEET In-Pile Ultrasonic Sensor Enablement-Final Report.” INL/EXT-14-32505, Idaho National Laboratory. https://doi.org/10.2172/1166037.

22. Zhang, Q., M. Chen, H. Liu, X. Zhao, X. Qin, F. Wang, Y. Tang, K. H. Yeoh, K.-H. Chew, X. Sun, 2021. “Deposition, characterization, and modeling of scandium-doped aluminum nitride thin film for piezoelectric devices.” *Materials* 14, no. 21 (2021): 6437. https://doi.org/10.3390/ma14216437.

23. Fourmentel, D., et al., “Acoustic sensor for in-pile fuel rod fission gas release measurement.*” IEEE Transactions on Nuclear Science*, vol 58, no. 1, pp. 151-155, 2011.

24. Phani, K. K., D. Sanyal, A. K. Sengupta, “Estimation of elastic properties of nuclear fuel material using longitudinal ultrasonic velocity – A new approach.” *Journal of Nuclear Materials* 366, no. 1-2 (2007): 129-136.

25. Prowant, M., et al., “Preliminary Design of High Temperature Ultrasonic Transducers for Liquid Sodium Environments, in Review of Progress in Quantitative Nondestructive Evaluation.” 2017: Provo, UT.

26. Parks, D. A., B. R. Tittmann, “Radiation tolerance of piezoelectric bulk single-crystal aluminum nitride.” *IEEE Transactions on Ultrasonics, Ferroelectrics, and Frequency Control*, vol. 61, no. 7, pp. 1216-1222, 2014.

27. Genenko, Y. A., et al., “Mechanisms of aging and fatigue in ferroelectrics.” *Materials Science and Engineering: B* 192 (2015): 52-82.

28. Glaum, J., et al., “De-aging of Fe-doped lead-zirconate-titanate ceramics by electric field cycling: 180°- vs. non-180° domain wall processes.” *J. Appl. Phys.*, 2012. **112**(3): p. 034103. https://doi.org/10.1063/1.4739721.

29. Gotmare, S. W., S. O. Leontsev, R. E. Eitel, “Thermal Degradation and Aging of High-Temperature Piezoelectric Ceramics.*” Journal of the American Ceramic Society*, 2010. **93**(7): 965-1969.

30. Berger, L. 1997. “*Semiconductor Materials*.” CRC Press.

31. Kazys, R., A. Voleisis, R. Sliteris, L. Mazeika, R. Van Nieuwenhove, P. Kupschus, H. A. Abderrahim, “High temperature ultrasonic transducers for imaging and measurements in a liquid Pb/Bi eutectic alloy.” *IEEE Transactions on Ultrasonics, Ferroelectrics, and Frequency Control*, vol. 52, no. 4, pp. 525–537, 2005. https://doi.org/10.1109/TUFFC.2005.1428033.

32. Trachenko, K., 2004. “Understanding resistance to amorphization by radiation damage.” *J. Phys.: Condens Matter* 16, no. 49: R1491–R1515. https://doi.org/10.1088/0953-8984/16/49/R03.

33. Reinhardt, B., B. Tittmann, J. Rempe, J. Daw, G. Kohse, D. Carpenter, M. Ames, Y. Ostrovsky, P. Ramulhalli, H. Chien. 2014. “Progress towards developing neutron tolerant magnetostrictive and piezoelectric transducers.” *AIP Conference Proceedings* 1650, no. 1, 1512 (2014). https://doi.org/10.1063/1.4914769.

34. Tittmann, B. R., C. F. G. Batista, Y. P. Trivedi, C. J. Lissenden III, B. T. Reinhardt. 2019. “State-of-the-Art and Practical Guide to Ultrasonic Transducers for Harsh Environments Including Temperatures above 2120 °F (1000°C) and Neutron Flux above 10^{13} n/cm^2.” *Sensors* 19(21): 4755. https://doi.org/10.3390/s19214755.

35. Primak, W., T. Anderson. 1975. “Metamictization of Lithium Niobate by Thermal Neutrons.” Nuclear Technology 23: 235. https://doi.org/10.13182/NT76-A31564.

36. Wong, K. 2002. “*Properties of Lithium Niobate*.” (No. 28) IET.

37. Zhang, S., F. Yu. 2011. “Piezoelectric Materials for High Temperature Sensors.” Journal of the American Ceramic Society 94(10), 3153–3170: 2011. https://doi.org/10.1111/j.1551-2916.2011.04792.x.

38. Meleshko, Y. P., S. G. Karpechko, G. K. Leont'ev, V. I. Nalivaev, A. D. Nikiforov, V. M. Smirnov, 1986, “Radiation Resistance of the Piezoelectric Ceramics TrsTS-21 and TNV-I,” Translated from Atomnaya Energiya: 50-52.

39. Jagadish, C., S. J. Pearton. 2006. “Zinc Oxide Bulk, Thin Films and Nanostructures: Processing, Properties, and Applications,” Elsevier. https://doi.org/10.1016/B978-0-08-044722-3.X5000-3.

40. Zhang, S., Y. Fei, B. H. T. Chai, E. Frantz, D. W. Snyder, X. Jiang, T. R. Shrout. 2008. “Characterization of piezoelectric single crystal YCa4O (BO3)3 for high temperature applications.” *Applied Physics Letters* 92(20) 202905 (2008). https://doi.org/10.1063/1.2936276.

41. Glass, S. W., J. P. Lareau, K. S. Ross, S. Ali, F. Hernandez, B. Lopez. 2019. “Magnetostrictive cold spray sensor for harsh environment and long-term condition monitoring.” *AIP Conference Proceedings* 2102(1) 020018: (2019). https://doi.org/10.1063/1.5099722.

42. Vinogradov, S., T. Eason, M. Lozev, (February 20, 2018). “Evaluation of Magnetostrictive Transducers for Guided Wave Monitoring of Pressurized Pipe at 200°C.” *ASME. J. Pressure Vessel Technol.* Apr 2018; 140(2): 021603. https://doi.org/10.1115/1.4038726.

43. Vinogradov, S., Jay L. Fisher, (2019). “New Magnetostrictive Transducers and Applications for SHM of Pipes and Vessels.” American Society of Mechanical Engineers Digital Collection.

44. Wang, Qian, Mingming Li, Xiaodong Niu, Mengfei Liu, Bowen Wang. “Model and Design of High-Temperature Ultrasonic Sensors for Detecting Position and Temperature Based on Iron-Based Magnetostrictive Wires.” *IEEE Sensors Journal*, vol. 21, no. 23, pp. 26868–26877, 2021. https://doi.org/10.1109/JSEN.2021.3119895.

45. Burrows, S. E., Y. Fan, S. Dixon. 2014. “High temperature thickness measurements of stainless steel and low carbon steel using electromagnetic acoustic transducers.” NDT & E International 68: 73–77. https://doi.org/10.1016/j.ndteint.2014.07.009.

46. Quintero, R., F. Simonetti, P. Howard, J. Friedl, and A. Sellinger. 2017. “Noncontact Laser Ultrasonic Inspection of Ceramic Matrix Composites (CMCs).” NDT & E International, vol. 88, pp. 8–16, 2017. https://doi.org/10.1016/j.ndteint.2017.02.008.

47. Matsumoto, T., T. Nose, Y. Nagata, K. Kawashima, T. Yamada, H. Nakano, S. Nagai. 2001. "Measurement of High-Temperature Elastic Properties of Ceramics Using a Laser Ultrasonic Method." Journal of the American Ceramic Society 84(7): 1521–1525. https://doi.org/10.1111/j.1151-2916.2001.tb00871.x.

48. Yu, F., O. Saito, Y. Okabe. 2021. "An ultrasonic visualization system using a fiber-optic Bragg grating sensor and its application to damage detection at a temperature of 1000°C." Mechanical Systems and Signal Processing 147: 107140. https://doi.org/10.1016/j.ymssp.2020.107140.

49. Morgan, B. W., M. P. Van Zile, C. M. Petrie, P. Sabharwall, M. Burger, I. Jovanovic. 2022. "Optical Absorption of Fused Silica and Sapphire Exposed to Neutron and Gamma Radiation with Simultaneous Thermal Annealing." Journal of Nuclear Materials 570: 153945. https://doi.org/10.1016/j.jnucmat.2022.153945.

50. Prasad, V. S. K., Krishnan Balasubramaniam, Elankumaran Kannan, K. L. Geisinger, "Viscosity Measurements of Melts at High Temperatures Using Ultrasonic Guided Waves." *Journal of Materials Processing Technology* 207(1–3), 2008: 315–320, ISSN 0924-0136. https://doi.org/10.1016/j.jmatprotec.2008.06.049.

51. Wei, Yanlong, Yubin Gao, Zhaoqian Xiao, Gao Wang, Miao Tian, Haijian Liang. 2016. "Ultrasonic Al2O3 Ceramic Thermometry in High-Temperature Oxidation Environment." *Sensors* 2016, **16**(11): 1905. https://doi.org/10.3390/s16111905.

52. Periyannan, Suresh, Prabhu Rajagopal, Krishnan Balasubramaniam. 2017. "Ultrasonic bent waveguides approach for distributed temperature measurement." *Ultrasonics* 74 (2017): 211–220. https://doi.org/10.1016/j.ultras.2016.10.015.

53. Cheong, Yong-Moo, Kyung-Mo Kim, Dong-Jin Kim. "High-temperature ultrasonic thickness monitoring for pipe thinning in a flow-accelerated corrosion proof test facility." *Nuclear Engineering and Technology* 49, no. 7 (2017):1463–71. https://doi.org/10.1016/j.net.2017.05.002.

54. Kogia, Maria, Tat-Hean Gan, Wamadeva Balachandran, Makis Livadas, Vassilios Kappatos, Istvan Szabo, Abbas Mohimi, Andrew Round. 2016. "High Temperature Shear Horizontal Electromagnetic Acoustic Transducer for Guided Wave Inspection." *Sensors* 16(4): 582. https://doi.org/10.3390/s16040582.

55. Baillie, I., P. Griffith, X. Jian, S. Dixon. 2007. "Implementing an Ultrasonic Inspection System to Find Surface and Internal Defects in Hot, Moving Steel Using EMATs." *Insight - Non-Destructive Testing and Condition Monitoring* 49(2): 87–92. https://doi.org/10.1784/insi.2007.49.2.87.

56. Reinhardt, B., J. Daw, B. R. Tittmann. "Irradiation Testing of Piezoelectric (Aluminum Nitride, Zinc Oxide, and Bismuth Titanate) and Magnetostrictive Sensors (Remendur and Galfenol)." *IEEE Transactions on Nuclear Science*, vol 65, no. 1, pp. 533–738, 2018. https://doi.org/10.1109/TNS.2017.2775163.

57. Tezuka, Kenichi, Michitsugu Mori, Sanehiro Wada, Masanori Aritomi, Hiroshige Kikura, Yukihiro Sakai. 2008. "Analysis of ultrasound propagation in high-temperature nuclear reactor feedwater to investigate a clamp-on ultrasonic pulse doppler flowmeter." *Journal of Nuclear Science and Technology* 45(8):752–762. https://doi.org/10.1080/18811248.2008.9711476.

58. Bilgunde, P. N., L. J. Bond, "Effect of Thermal Degradation on High Temperature Ultrasonic Transducer Performance in Small Modular Reactors." *Physics Procedia* 70, (2015): 433-436. https://doi.org/10.1016/j.phpro.2015.08.137.

59. Honarvar, Farhang, Farzaneh Salehi, Vahid Safavi, Arman Mokhtari, Anthony N. Sinclair. "Ultrasonic monitoring of erosion/corrosion thinning rates in industrial piping systems." *Ultrasonics* 53, no. 7 (2013): 1251–1258. https://doi.org/10.1016/j.ultras.2013.03.007.

60. Kazys, Rymantas, Reimondas Sliteris, Regina Rekuviene, Egidijus Zukauskas, Liudas Mazeika. 2015. “Ultrasonic Technique for Density Measurement of Liquids in Extreme Conditions.” *Sensors* 2015, **15**(8): 19393–415.

61. Fei, Chunlong, et al. “0.36BiScO3-0.64PbTiO3 Piezoelectric Ceramics for High Temperature Ultrasonic Transducer Applications.” *Journal of Alloys and Compounds* 743, (2018): 365–371, ISSN 0925-8388. https://doi.org/10.1016/j.jallcom.2018.01.393.

62. Cegla, F. B., A. J. C. Jarvis, J. O. Davies. “High Temperature Ultrasonic Crack Monitoring Using SH Waves.” NDT & E International 44, no. 8, (2011): 669–79. https://doi.org/10.1016/j.ndteint.2011.07.003.

63. Cegla, F. B., P. Cawley, J. Allin, J. Davies. “High-Temperature (>500°c) Wall Thickness Monitoring Using Dry-Coupled Ultrasonic Waveguide Transducers.” *IEEE Transactions on Ultrasonics, Ferroelectrics, and Frequency Control*, vol. 58, no. 1, 156–167, 2011. https://doi.org/10.1109/TUFFC.2011.1782.

64. Amini, M. H., A. N. Sinclair, T. W. Coyle. “A New High-Temperature Ultrasonic Transducer for Continuous Inspection.” *IEEE Transactions on Ultrasonics, Ferroelectrics, and Frequency Control*, vol. 63, no. 3, 448–55, 2016. https://doi.org/10.1109/TUFFC.2016.2519348.

65. Balasubramaniam, Krishnan, Vimal V. Shah, R. Daniel Costley, Gary Boudreaux, Jagdish P. Singh. 1999. “High Temperature Ultrasonic Sensor for the Simultaneous Measurement of Viscosity and Temperature of Melts.” *Review of Scientific Instruments* **70,** no. 12, 4618–4623 (1999). https://doi.org/10.1063/1.1150123.

66. Hernandez-Valle, Francisco, Steve Dixon. “Initial Tests for Designing a High Temperature EMAT with Pulsed Electromagnet.” NDT & E International 43, no. 2, (2010):171–175. https://doi.org/10.1016/j.ndteint.2009.10.009.

67. Kogia, M., et al. 2015. “Electromagnetic Acoustic Transducers Applied to High Temperature Plates for Potential Use in the Solar Thermal Industry.” *Appl. Sci.* 2015, 5(4), 1715–1734. https://doi.org/10.3390/app5041715.

68. Lunn, N., S. Dixon, M. D. G. Potter. “High Temperature EMAT Design for Scanning or Fixed Point Operation on Magnetite Coated Steel.” NDT & E International 89. (2017): 74–80. https://doi.org/10.1016/j.ndteint.2017.04.001.

69. Zhai, Guofu, Bao Liang, Xi Li, Yuhang Ge, Shujuan Wang. 2022. “High-Temperature EMAT with Double-Coil Configuration Generates Shear and Longitudinal Wave Modes in Paramagnetic Steel.” NDT & E International 125, (2022): 102572. https://doi.org/10.1016/j.ndteint.2021.102572.

70. Hernandez-Valle, F., S. Dixon. “Pulsed Electromagnet EMAT for Ultrasonic Measurements at Elevated Temperatures.” *Insight - Non-Destructive Testing and Condition Monitoring*, vol. 53, no. 2, 1 Feb 2011, pp 96–99. https://doi.org/10.1784/insi.2011.53.2.96.

71. Ogata, Shohei, Tetsuya Uchimoto, Toshiyuki Takagi, Gerd Dobmann. 2018. “Development and Performance Evaluation of a High-Temperature Electromagnetic Acoustic Transducer for Monitoring Metal Processing.” *International Journal of Applied Electromagnetics and Mechanics*, vol. 58, no. 3, pp. 309–318, 2018. https://doi.org/10.3233/JAE-180016.

72. Ren, Weiping, Ke Xu, Steve Dixon, Chu Zhang. 2019. “A Study of Magnetostriction Mechanism of EMAT on Low-Carbon Steel at High Temperature.” NDT & E International 101 (2019): 34–43. https://doi.org/10.1016/j.ndteint.2018.10.001.

73. Ueno, T., T. Higuchi, 2005. “High Sensitive and heat-resistant magnetic sensor using magnetostrictive/piezoelectric laminate composite.” in *IEEE Transactions on Magnetics*, vol. 41, no. 10, pp. 3670–72, Oct. 2005. https://doi.org/10.1109/TMAG.2005.854795.

74. Ueno, Toshiyuki, Toshiro Higuchi. 2005. “Magnetic Sensor for High Temperature Using a Laminate Composite of Magnetostrictive Material and Piezoelectric Material.” in Smart Structures and Materials 2005: Active Materials: Behavior and Mechanics. **5761**: 156–63 SPIE.

75. Pernía, Alberto M., Héctor Andrés Mayor, Miguel J. Prieto, Pedro J. Villegas, Fernando Nuño, Juan A. Martín-Ramos. 2019. “Magnetostrictive Sensor for Blockage Detection in Pipes Subjected to High Temperatures.” *Sensors* **19**(10): 2382. https://doi.org/10.3390/s19102382.

76. Vinogradov, Sergey, Thomas Eason, Mark Lozev. 2018. “Evaluation of Magnetostrictive Transducers for Guided Wave Monitoring of Pressurized Pipe at 200°C.” *ASME. J of Pressure Vessel Techno.* April 2018; **140(**2): 021603. https://doi.org/10.1115/1.4038726.

77. Vinogradov, Sergey, Jay L. Fisher. 2019. “New Magnetostrictive Transducers and Applications for SHM of Pipes and Vessels.” American Society of Mechanical Engineers Digital Collection.

78. Fraizier, E., M. H. Nadal, R. Oltra. 2002. “Evaluation of Viscoelastic Constants of Metallic Materials by Laser-Ultrasonics at Elevating Temperature.” *Ultrasonics* 40**,** no. 1 (2002): 543–47. https://doi.org/10.1016/S0041-624X(02)00165-8.

79. Lee, Hyeonseok, Jinyeol Yang, Hoon Sohn. 2012. “Baseline-Free Pipeline Monitoring Using Optical Fiber–Guided Laser Ultrasonics.” *Structural Health Monitoring* **11(**6), 684–95. https://doi.org/10.1177/1475921712455682.

80. Yang, Jinyeol, Hyeonseok Lee, Hyung Jin Lim, Nakhyeon Kim, Hwasoo Yeo, Hoon Sohn. 2013. “Development of a Fiber-Guided Laser Ultrasonic System Resilient to High Temperature and Gamma Radiation for Nuclear Power Plant Pipe Monitoring.” *Meas. Sci. Technol.*, **24**(8): 085003. https://doi.org/10.1088/0957-0233/24/8/085003.

81. Zamiri, Saeid, Bernhard Reitinger, Hubert Grün, Jürgen Roither, Siegfried Bauer, Peter Burgholzer. “Laser Ultrasonic Velocity Measurement for Phase Transformation Investigation in Titanium Alloy,” in *2013 IEEE International Ultrasonics Symposium (IUS)*. 2013, pp. 683-686. https://doi.org/10.1109/ULTSYM.2013.0176.

82. Burgess, K., V. Prakapenka, E. Hellebrand, aP. V. Zinin. “Elastic characterization of platinum/rhodium alloy at high temperature by combined laser heating and laser ultrasonic techniques.” *Ultrasonics* 54, no. 4, (2014): 963–966. https://doi.org/10.1016/j.ultras.2014.01.011.

83. Klose, Joshua, Sarah Esch, Peter Kohns, Georg Ankerhold. “Assessment of the intrinsic damage to refractory materials at high temperatures using the laser ultrasonic pulse method.” *Open Ceramics*, 9, (2022): 100221. https://doi.org/10.1016/j.oceram.2022.100221.

84. Rodrigues, Mariana C. M., Thomas Garcin, Matthias Militzer. “In-Situ measurement of α formation kinetics in a metastable β ti-5553 alloy using laser ultrasonics.” *Journal of Alloys and Compounds*, vol. 866 (2021):158954. https://doi.org/10.1016/j.jallcom.2021.158954.

85. Kosugi, Akira, Ikuo Ihara, Iwao Matsuya. “Accuracy Evaluation of Surface Temperature Profiling by a Laser Ultrasonic Method.” *Jpn. J. Appl. Phys.*, vol. 51 (2012): 07GB01. https://doi.org/10.1143/JJAP.51.07GB01.